

Studying the Factors Affecting the Drag Coefficient in Non-Newtonian Fluids

Muhammad A. R. Mohammed and Dina Adil Elia Halagy

Chemical Engineering Department, College of Engineering, University of Nahrain

Abstract

The aim of this research is to study the factors affecting drag coefficient (C_d) in non-Newtonian fluids which are the rheological properties, concentrations of non-Newtonian fluids, particle shape, size and the density difference between particle and fluid. Also this study shows drag coefficient (C_d) and particle Reynolds' number (Re_p) relationship and the effect of rheological properties on this relationship.

An experimental apparatus was designed and built, which consists of Perspex pipe of length of 160 cm. and inside diameter of 7.8 cm. to calculate the settling velocity, also electronic circuit was designed to calculate the falling time of particles through fluid.

Two types of solid particles were used; glass spheres and crushed rocks as irregularly shaped particles with different diameters and compared with each other. The concept of equivalent spherical diameter (D_s) was used to calculate the diameters of irregularly shaped particles.

The flow behavior for Non-Newtonian fluids was represented by Power-Law model. Two types of polymers were used, Carboxy Methyl Cellulose CMC with concentrations of (3.71, 5, 15 and 17.5) g/l and polyacrylamide with concentrations of (2, 4 and 6) g/l.

The results showed that the drag coefficient decreased with increasing settling velocity and particle diameters and sizes; and increased as fluid become far from Newtonian behavior and concentrations and the density difference between particle and fluid.

The results also showed that the rheological properties of Non-Newtonian fluids have a great effect on the drag coefficient and particle Reynolds number relationship, especially in laminar-slip regime and decreases or vanishes at transition and turbulent-slip regimes.

New correlations were obtained which relates drag coefficient with concentrations of polymers and with flow behavior indices for spherical and irregular shaped particles in Carboxy Methyl Cellulose CMC and polyacrylamide solutions.

Keywords: Fluid flow, Drag, Settling.

Introduction

It has been shown theoretically and experimentally that the resisting force

acting on a body moving in a fluid depends on particle's shape, size, projected area, the relative velocity of

the body, and on the density and viscosity of the fluid [1].

The terminal settling velocity is the most important factor, which affecting relationship between the drag coefficient and particle Reynolds' number, since it is involving in the evaluation of these two quantities [2].

In 1959, Becker [3] stated that the drag on oriented bodies (or particles) in motion through an infinite fluid is composed of a viscous drag and an inertial drag, in which a quadratic drag formula was adopted. This drag is related to the fluid velocity and to properties of the fluid and the particle. According to that drag is related to particle Reynolds' number.

The first attempt is made by Slattery and Bird in 1961 [4], to understand the behavior of non-Newtonian fluid around particles. They used Ellis rheological model in their study, and they measured the drag coefficient of spheres moving through CMC solutions. Two dimensionless correlations for drag coefficient in terms of a modified particle Reynolds' number based on Ellis parameters, have been adopted.

The first study on a modified C_d - Re_p relationship for sphere in Bingham Plastic non-Newtonian fluid is conducted by Valentick and Whitmore [5] in 1965. They used a flocculated aqueous clay suspension of six densities with different flow parameters. These suspensions follow Bingham Plastic model. They stated that the drag forces of a particle moving in Bingham fluid are composed of force of falling in Newtonian fluid and a force to overcome the yield stress of Bingham Plastic.

Particle Dynamics

The movement of a particle through a fluid requires external force acting on

a particle. This force may come from a density difference between the particle and the fluid or may be the result of electric or magnetic fields.

Three forces act on a particle moving through a stagnant fluid: The gravitational (F_G), the buoyant force (F_B) which acts parallel with the external force but in opposite direction and the drag force (F_D) which appears whenever there is relative motion between the particle and the fluid. The drag force acts to oppose the motion and acts parallel with direction of movement but in opposite direction, as shown in figure 1 [6, 7].

Drag coefficient may be calculated from:

$$C_d = \frac{4}{3} \frac{D_s(\rho_p - \rho_f)}{\rho_f V_s^2} g \quad \dots (1)$$

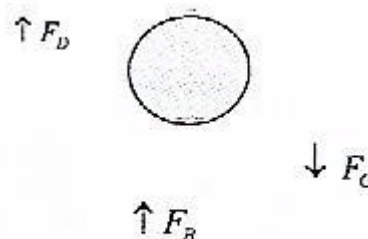


Fig. 1 A free falling particle under the action of gravity [3]

Particle Reynolds' Number, Re_p

Particle Reynolds' number is used to indicate whether the boundary layer around a particle is turbulent or laminar, and the drag exerted will depended on this. It is a measure of the relative important of inertial to viscous forces of flow [8], and is given by their ratio by following formula:

$$Re_p = \frac{\rho_f V_s D_p}{\mu} \quad \dots (2)$$

For Newtonian fluid, viscosity μ is constant independent of shear rate and the concept settling shear rate is not used [2].

For Non-Newtonian fluid the viscosity varies with the shear rate. Therefore, an expression of equivalent viscosity μ_{eq} can be used, which represent the viscosity of fluid around the particle during its movement. The equivalent viscosity is defined as the ratio of shear stress on particle surface to average shear rate of the particle [2].

$$\mu_{eq} = 478.8 \frac{\tau_p}{\gamma_p} \quad \dots (3)$$

There are several equations that relate shear stress to shear rate for non-Newtonian fluids.

According to that, there are several forms of equivalent viscosities depending on the type of the non-Newtonian model. In this study power-law model's equation is only used and the equivalent viscosity of this model as follows [2]:

$$\mu_{eq} = 478.8K \left(0.6 \frac{V_s}{D_p}\right)^{n-1} \quad \dots (4)$$

Experimental Apparatus and Materials

An experimental apparatus has been designed and built to measure the terminal settling velocity for solid particles so drag coefficient and particle Reynolds' number can be calculated. The test apparatus is consisting of vertical and transparent Perspex pipe, with length of 160 cm, outside diameter of 8 cm and inside diameter of 7.8 cm to avoid wall effects as shown in figure (2) below.

For careful determination of terminal settling velocity the pipe was divided into four sections as follows;

1. First section is inlet section L1. It is used for acceleration which defined

as the distance that particle should travel before reaching an equilibrium of forces to get constant velocity (settling velocity). The first section must have sufficient settling length for accurate timing, so the inlet length used in this work was 85 cm.

2. Second section is test section L2. It is used for calculating the terminal settling velocity. The length was 50 cm, this section divided into two sections each of them 25 cm.
3. The third section is Drainage section L3. It is used for draining the fluid and avoids end effects

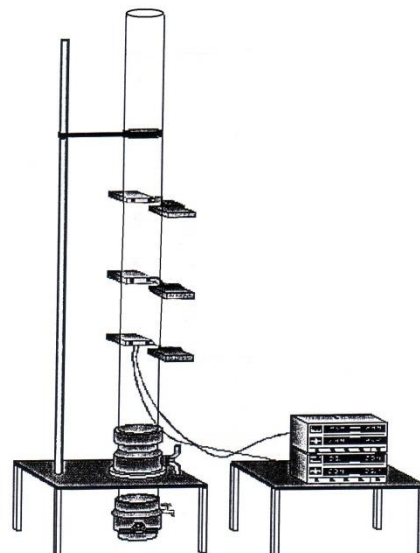


Fig. 2, Schematic diagram for experimental apparatus

Electrical Circuit

The precision of measurement of the velocity is directly related to the time taken by the particle to travel a known distance (after travel L1). Aiming to assure the precision of the time measurement and to eliminate the human error, a digital electronic circuit was designed with three photo-sensor nets; these three nets are measured the time of particle falling in test section through fluid.

The transmitter transmits an Infa-Red ray to five receivers, when particle fell down through the column and reaches

distance of 85 cm the ray will disconnect.

The designs of the counter's circuit, transmitters and receivers are shown in figs. 3a, 3b and 4.

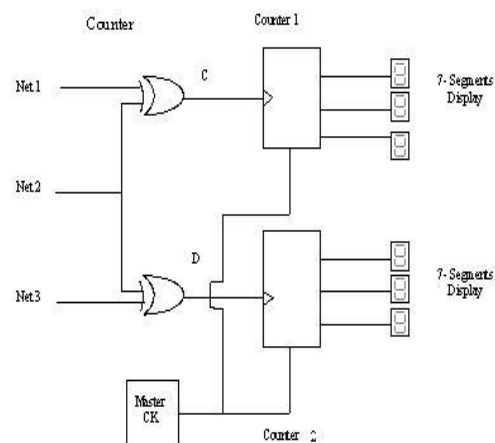


Fig. 3a, design of counter's circuit

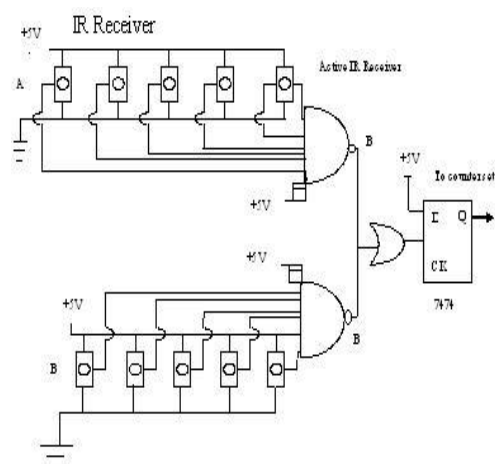


Fig. 3b, design of counter's circuit

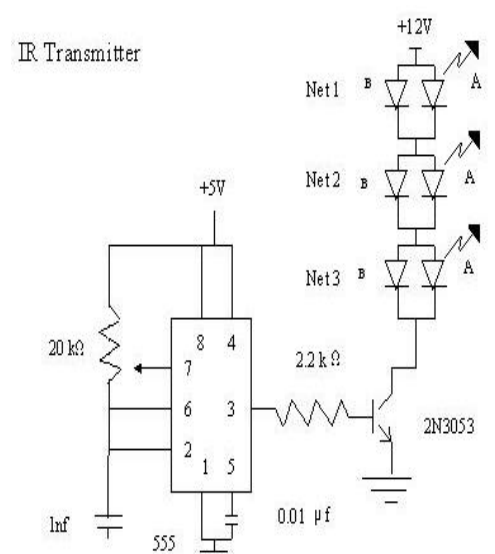


Fig. 4, The design of the transmitter

Test Fluids

In order to get different rheological properties two polymers were used, Carboxy Methyl Cellulose CMC and polyacrylamide (Water Soluble Polymers) with different concentrations as non-Newtonian fluids and water as Newtonian fluid. Seven different concentrations were prepared, four for CMC and three for polyacrylamide, these values are given in table (1).

The densities of each test fluids used in this experimental work have been measured by pycnometer of volume 25 ml. The density of all polymer solutions prepared found to be 1 gm./cc. Power-Law model was used to represent the flow behavior of non-Newtonian fluids. The rheological properties (n, k) of each non-Newtonian fluid used for settling velocity determinations were measured by Fann VG meter model 35A rotational coaxial cylinder type. The parameters n and k can be determined approximately using a Fann-VG reading as follow;

$$n = 3.32 \log \frac{\theta_{600}}{\theta_{300}}$$

$$k = \frac{\theta_{600}}{(1022)^n}$$

Where; θ_{600} = dial reading at 600 rpm, and; θ_{300} = dial reading at 300 rpm

Particle Diameter's Measurements

a. Sphere Particles

Spherical particles are made of glass with different diameters; the diameters were measured by a vernier with an accuracy of 0.01 mm. The weight of particles was measured by a digital balance and the volume was calculated using

$$\text{Vol.} = \frac{\pi}{6} D_s^3, \text{ while the area} = \frac{\pi}{4} D_s^2$$

Then, the density of the particle is the ratio of its weight to its volume; the physical characteristics of spherical particles are given in table 2.

b. Irregular Shaped Particles

The irregular shaped particles are formed from crushed rocks. The problem with these particles that they do not have standard diameters, so the concept of the equivalent spherical diameter D_s was used, which represented the diameter has a volume of sphere.

The volume of irregular shaped particles had been measured by displacement method using Kerosene; physical characteristics of irregular particles are given in table 3.

Table 1, Concentrations of polymers and Power-Law constants

No.	Polymer	Concentration, g./l	Power-Law constants
1	CMC	3.71	n=0.73,k=0.015
2	CMC	5	n=0.71,k=0.091
3	CMC	15	n=0.63,k=0.287
4	CMC	17.5	n=0.61,k=0.566
5	Polyacr.	2	n=0.58,k=1.016
6	Polyacr.	4	n=0.51,k=1.135
7	Polyacr.	6	n=0.39,k=3.320

Table 2, Physical characteristics of spherical particles

D_s ,cm.	Mass, g.	V_p , cm^3	ρ_p , $g./cm^3$	A_p , cm^2
0.22	0.014	0.0055	2.545	0.038
0.3	0.034	0.0141	2.411	0.071
0.4	0.082	0.033	2.484	0.126
0.6	0.299	0.113	2.646	0.283
0.8	0.675	0.268	2.518	0.503
1	1.338	0.524	2.553	0.785
1.43	3.825	1.531	2.498	1.606
2	10.841	4.189	2.588	3.141

Table 3, Physical characteristics of irregular shaped particles

D_s ,cm.	Mass, g.	V_p , cm^3	ρ_p , $gr./cm^3$	A_p , cm^2
0.984	0.970	0.5	1.940	0.762
1.102	1.554	0.7	2.220	0.954
1.152	1.862	0.8	2.327	1.042
1.198	1.936	0.9	2.151	1.127
1.241	2.735	1	2.735	1.209
1.388	3.042	1.4	2.173	1.513
1.420	2.719	1.5	1.813	1.584
1.563	4.791	2	2.395	1.919
1.789	8.391	3	2.797	2.514
1.823	7.104	3.2	2.220	2.610
1.847	8.358	3.3	2.533	2.679
2.121	10.640	5	2.128	3.536

Procedure of Experimental Work

The shape of the particles has not been measured in this study.

In order to get accurate results, great attention must be paid to each of the followings:

1. Firstly, all the used particles were washed in water and dried in oven, in order to avoid the error reading from dirty particles.
2. The temperature of the fluid was recorded of each run by a thermometer. The temperature remained at a room temperature (27-28 C) therefore the fluid properties remained constant throughout the experiment.
3. The pipe was set exactly vertical by using a balance with a bubble, when the bubble in the center of the balance, that means, the pipe is in a vertical position.
4. 7 liters of each fluid was prepared in batches by shaker or mixer adding the necessary amounts of polymer in water.
5. After the test fluid prepared and the pipe was filled with a test fluid, a single particle was introduced into the top of the pipe. The particle should place in the center of the pipe just below the surface of the test fluid and leave it to settle freely.

6. The first inlet section L1 was neglected in order to ensure that the acceleration of particle is ended. When the particle crossed the test sections of L2, L3 the variation in signal will produce in each photo-sensor net as explained previously and the number of counts will appear in 7-segments displays in the board for each net, then the number of counts changed to time by multiplying with counters' factor, so the time required for falling particle in each sections L2, L3 will be known.
7. All particles dropped in same way and number of counts recorded. The falling times for each particle in test section (L2 and L3) were measured.
8. The terminal settling velocity of the particle is the measure of the total times along L2 and L3 that the particle required to settle through a known distance of 50 cm, which represented the total test section.
$$V_s = 50 / t$$
9. The time of falling of small spherical particles (0.2, 0.3) cm. was recorded manually by digital stop watch with accuracy of 0.01 sec. along test section of 50 cm, because the photo sensor nets were not sufficiently sensitive to record the passing of these particles.
10. The orientation of each falling particles were observed, to show the difference between the falling of spherical particles and irregular shaped particles.
11. Then the test fluid was drained by the valve in iron base and particles were released by the second valve at the end of cone, in order to pump another solution and repeat the measurements, and so on.
12. To minimize the error, each experiment repeated 3-4 times. An average time was used, thus average settling velocity was taken.

13. The effect of pipe wall on settling velocity was avoided by taking the ratio of particle diameter to pipe diameter less than or equals to 0.25.

Results and Discussion

The values of drag coefficient are high at low values of Reynolds' number, and as Reynolds' number increased the drag coefficient will decrease, due to fact that the viscous forces are dominated in laminar-slip regime. When this region is ended the transition-slip regime is started, the effect of Reynolds' number on drag coefficient is decreased, until the turbulent-slip regime is started and the drag coefficient will be constant value due to the fact that the inertial forces are dominate in this region and viscous forces will have a small effect. For this reason, the increase in Reynolds' number will not decrease the drag coefficient. It is obvious from figure (5) that as flow behavior index (n) decreased from unity the drag coefficient will increase for the same particle Reynolds' number Re_p , because the particle will settle at lower velocity; and this effect is greatly realized at low values of Reynolds' number.

Factors Affect Drag Coefficient

1. Settling Velocity

As the settling velocity of the particles increased the drag coefficient will decrease, because as the velocity increased the drag force exerted by fluid on the particle will be decreased so the drag coefficient will decrease, for spherical and irregular particles, as shown in figure (6).

2. Particle Diameter

The concept of equivalent sphere diameter has been used to calculate the diameter of irregular shaped particles. As the particle diameter increased the

drag coefficient will be decreased. Due to that as the particle diameter increases the velocity of particle will increase, since the drag force exerted on particle will be decreased, so the drag coefficient decreases. This is shown in figures (7).

3. Difference between Particle and Fluid Densities

As the difference between particle and fluid density ($\rho_P - \rho_F$) increased the drag coefficient will increase. This is shown in figure 8.

4. Concentration

To show the effect of concentration of polymers (Carboxy Methyl Cellulose CMC, polyacrylamide) on drag coefficient, graphs are plotted for particles settling in Carboxy Methyl Cellulose CMC solution with concentrations of (3.71, 5, 15, 17.5) g/l and polyacrylamide solution with concentrations of (2, 4, 6) g/l for spheres and irregular shaped particles. As concentration increased, the viscosity of fluid will increase and settling velocity will decrease, so the drag coefficient increases for all diameters of particles used, as shown in figure 9.

5. Rheological Properties

The relationships between flow behaviour indices and drag coefficient with particle diameters for both spherical and irregular shaped particles had been studied. It is clear that as the flow behaviour index increased and approached to unity the drag coefficient decreased, due to the increase in the settling velocity of particles, for all diameters of particles which have been used. This is shown in figure 10.

Empirical Equations for Drag Coefficient

1. A general formula was obtained for drag coefficient (Y) versus Carboxy Methyl Cellulose CMC and Polyacrylamide concentrations (X) from our experimental work for spherical particles and irregular shaped particles

$$\text{Log } Y = B \text{ Log } X + A$$

2. A general formula was obtained for drag coefficient (Y) versus flow behavior index (X) from our experimental work for spherical particles and irregular shaped particles

$$\text{Log } Y = B \text{ Log } X + A$$

Where A, B are the constants of equation depends on the shape, diameters of particles and flow behavior indices.

Conclusions

1. As particle Reynolds number increased the drag coefficient will decrease especially in laminar-slip regime until the drag coefficient reaches a constant value in turbulent-slip regime.
2. The particle size has a great effect on the drag coefficient, as the particle diameter or volume increased the drag coefficient will decrease since the settling velocity will increase.
3. The rheological properties of non-Newtonian fluids have a great effect on drag coefficient, because as the fluid became far from Newtonian behavior, (flow index n far from unity), the drag coefficient will be increased.
4. The difference in density between the particle and fluid affect the drag coefficient, as the difference increases the drag coefficient will increase. The concentrations of polymer fluids have effect on C, it was shown that as the concentration of fluid increased the drag coefficient will increase.

Nomenclature

Symbol	Meaning	Unit
A_P	Projected area of the particle in a plane perpendicular to the direction of the flow.	cm^2
C_d	Particle drag coefficient	dimensionless
D	Inside pipe diameter	cm
D_P	Particle diameter	cm
D_S	Diameter of particle has the same volume as a sphere	cm
F	Force	dyne
F_B	Bouncy force	dyne
F_D	Drag force	dyne
F_G	Gravity force	dyne
g	Acceleration due to gravity	cm/s^2
k	Power-Law consistency index	$\text{g.s}^n/100 \text{ cm}^2$
L	Length	cm
n	Power-Law flow behavior index	dimensionless
Re_P	Particle Reynolds' number	dimensionless
V_P	Solid particle volume	cm^3
V_S	Settling velocity	cm/s

Greek Symbols

Symbol	Meaning	Unit
$\theta_{300}, \theta_{600}$	Dial reading of Fann-VG meter rpm, at 300 and 600 rpm respectively	degrees
μ	Newtonian fluid viscosity	cp
μ_{eq}	Equivalent viscosity	cp
ρ_F	Density of fluid	g/cm^3
ρ_P	Density of particle	g/cm^3

References

1. Pettyjohn E.S. and Christiansen E.B. "Effect of particle shape on free settling rates of isometric particles"; Chem. Eng. Progress, 44(1948), 2.
2. Muhannad A.R. "The effect of particles shape and size and the rheological properties of non-Newtonian fluids on drag coefficient and particle Reynold's number relationship", Ph.D. Thesis, (1998).
3. Becker H.A. "The effects of shape and Reynolds' number on drag in the motion of a freely oriented body in an infinite fluid", The Cand. J. of Chem. Eng., April, (1959).
4. Slattery J.C. and Bird R.B. "Non-Newtonian flow past a sphere", Chem. Eng. Science vol.16 (1961).
5. Valentik L. and Whitmore R.L. "The terminal velocity of spheres in Bingham plastic", Brit. J. Appl. Phys. vol.16 (1965).
6. Flemmer R.L.C. and Banks C.L. "On the drag coefficient of a sphere", Powder Tech. 48 (1986).

7. Michell S. J., "Fluid and particle mechanics", Pergamon Press LTD., (1970) p. 288- 301.
8. Given on internet by Courtney K.Harris, "Sediment transport processes in coastal environments", (2003), at
a. <http://www.vims.edu/~ckharris/ms698-03/lecture-2pdf>
9. Chhabra, R.P. and Richardson, " Non-Newtonian flow in the process industries", Elsevier Publishing Ltd. (1999).
10. Fann Viscometer, Model 35A Manual.
<http://www.expotechusa.com/manuals/fann/35496.pdf>
11. Flinn Scientific Inc., "Preparation of polyvinyl alcohol" (2003).
12. Taugbol, K. , Fimreite, G. , O.I. , Svanes, K., Omland, T. H., Sveta, P. E., and Breivik, D .H., "Development and Field Testing of a Unique High-Temperature/High Pressure (HTHP) Oil-Based Drilling Fluid With Minimum Rheology and Maximum Sag Stability", SPE 96285, 2005.
13. Carbajal, D., Burress, C.,Shumway, B., and Zhang, Y., "Combining Proven Anti-Sag Technologies for HTHP North Sea Applications: Clay-Free Oil-Based Fluid and Synthetic, Sub-Micron Weight Material", SPE/IADC 119378, 2009

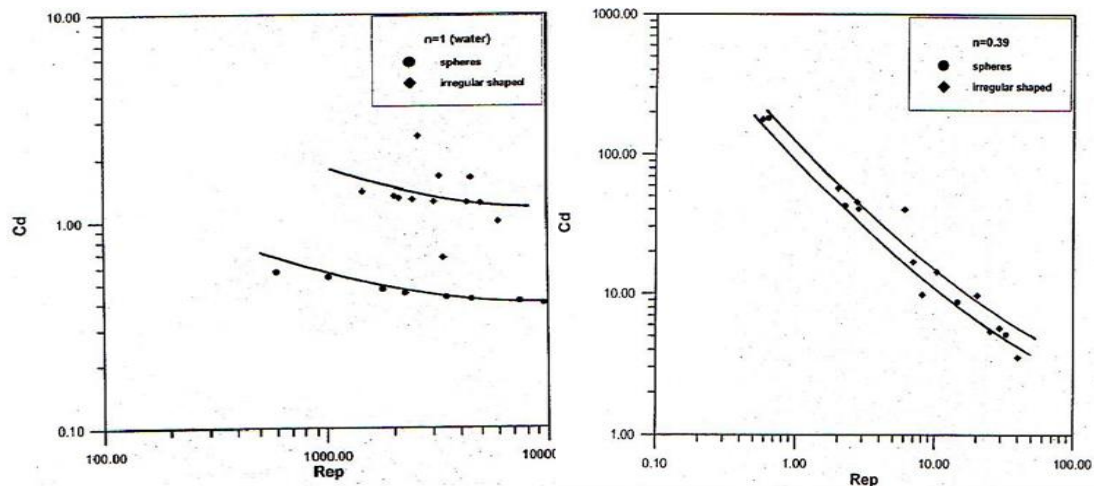


Fig. 5, $C_d - Re_p$ relationship at different flow behavior (n)

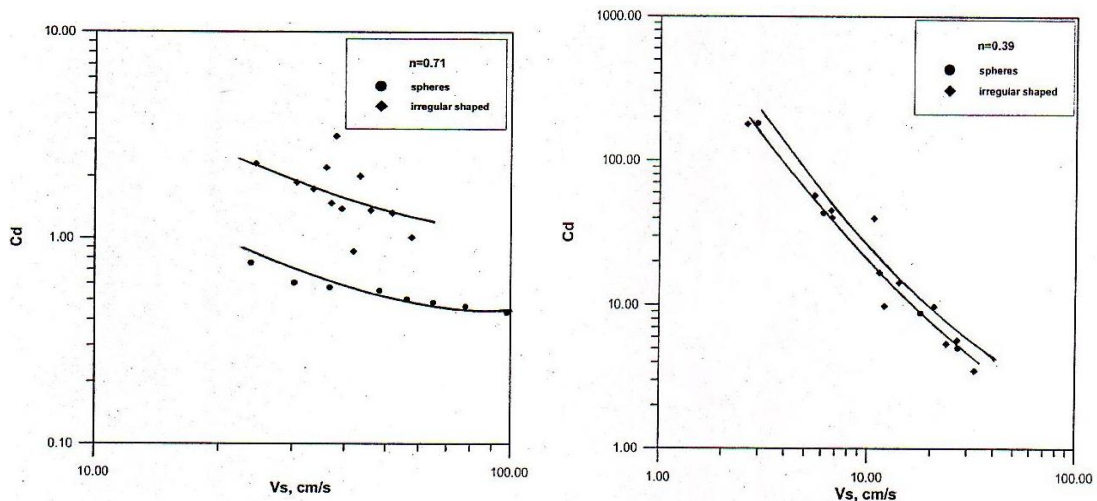


Fig. 6, The effect of terminal settling on drag coefficient

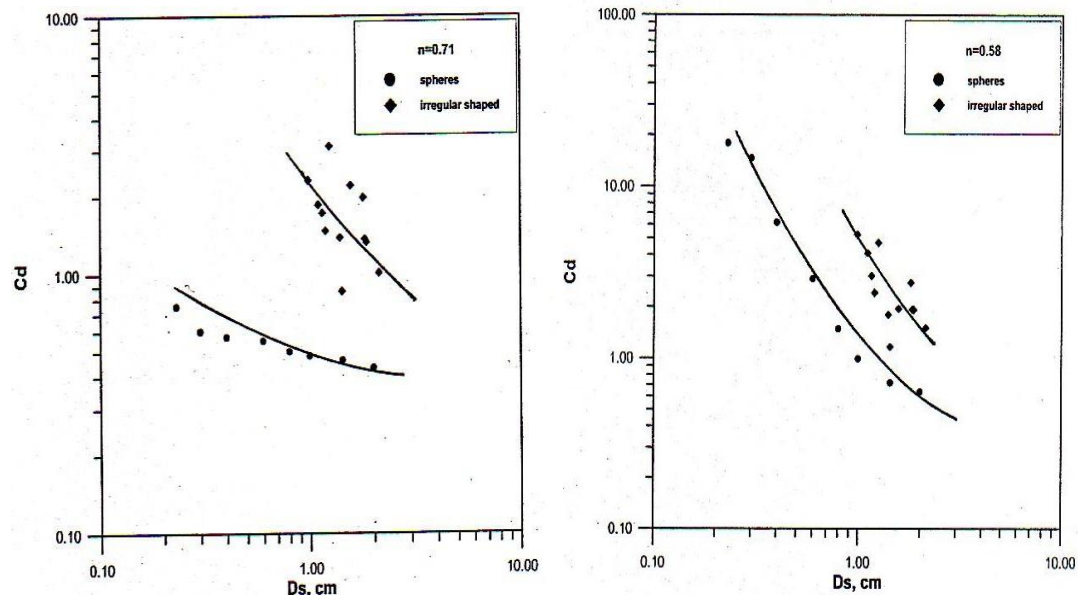


Fig. 7, The effect of particle diameter on drag coefficient

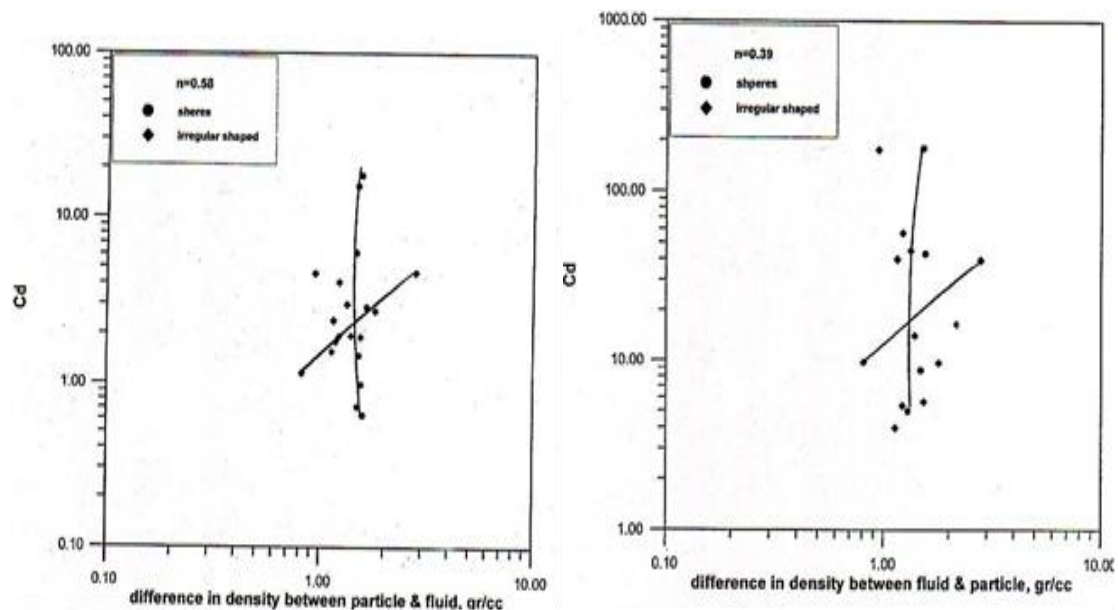


Fig. 8, The effect of difference in density between the particle and fluid on drag coefficient

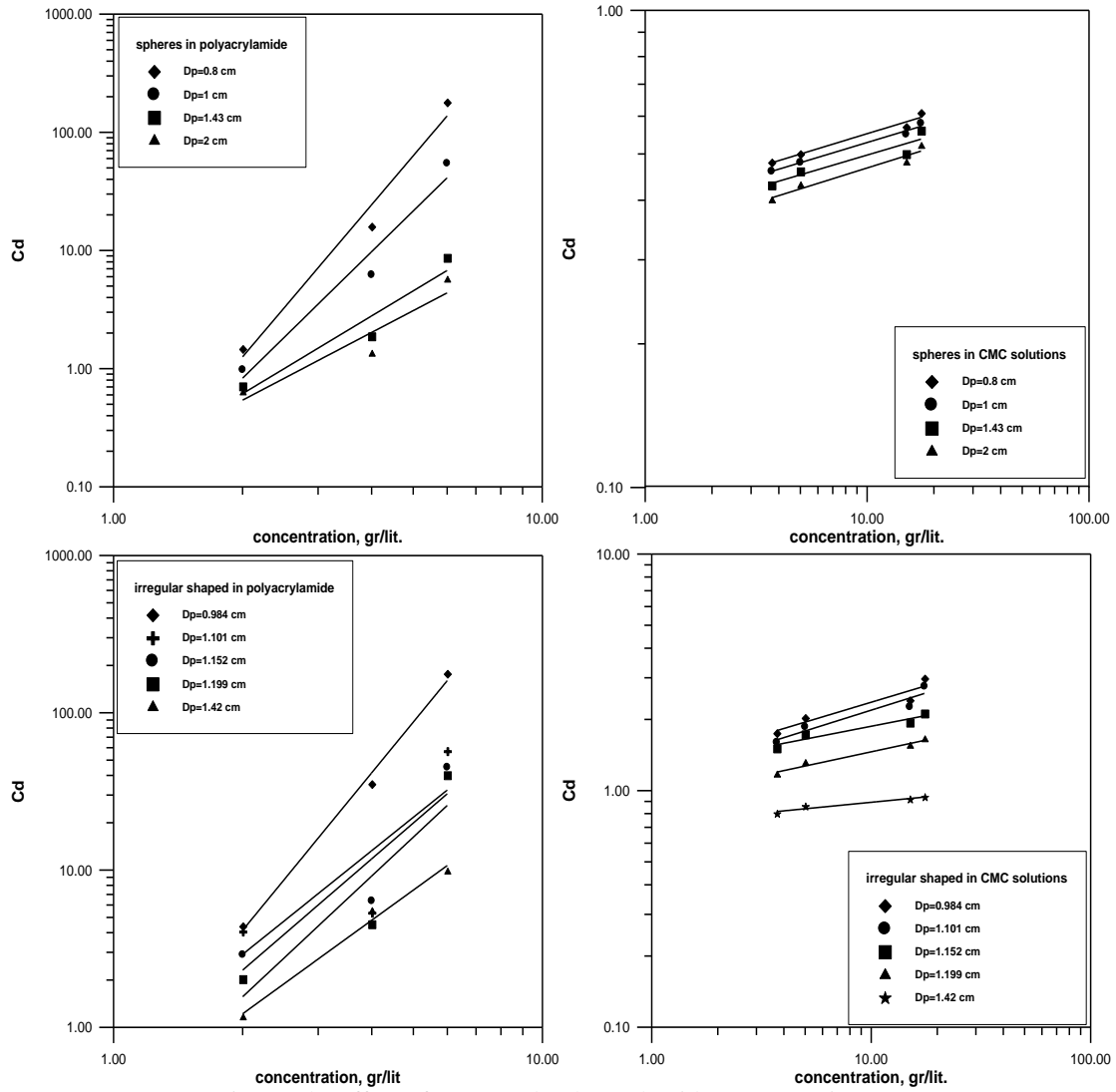


Fig. 9, The effect of CMC and polyacrylamide concentrations on C_d for different diameters of spherical and irregular shaped particles

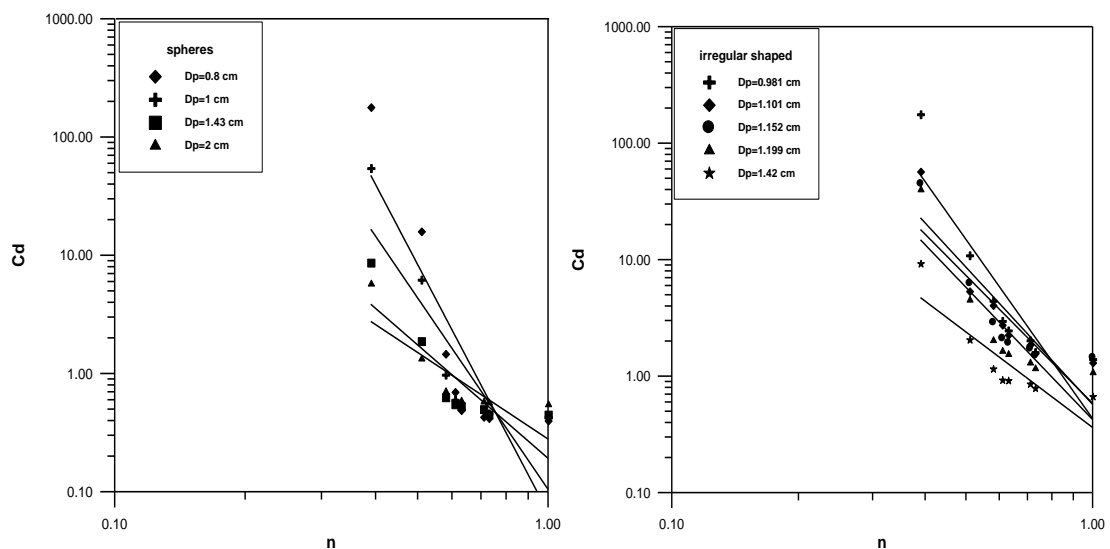


Fig. 10, The effect of flow index on C_d for different diameters of spherical and irregular shaped particles